Experimental investigation on low-carbon quenched and partitioned steel

E. Pastore, S. De Negri, M. Fabbreschi, M.G. Ienco, M.R. Pinasco, A. Saccone, R. Valentini

This work is part of a wider study concerning Q&P steels subjected to different thermal cycles. The Q&P processes were carried out on the Gleeble 3800 thermomechanical simulator. The steels investigated are identified as Si, Al and Mo steels. The first results, presented in this article, are relative to a silicon steel after quenching from different temperatures (always in the α+γ intercritical field), followed by partitioning at different temperatures and for different times. The aim of these treatments was to evaluate the influence of process parameters on the microstructure and consequently on the mechanical properties.
The microstructure was investigated by optical and scanning electron microscopy (SEM); the phases were identified by electron back scattered diffraction (EBSD); the volume fraction of retained austenite, at room temperature, was measured by X-ray diffraction; and HV hardness measurements were performed. Transmission electron microscopy (TEM) examinations are in progress. Some mechanical properties were measured by tensile tests. The mainly phases present in the microstructure of the steel were: ferrite, lath martensite and "retained" austenite. Their morphology and relative amounts depend on the thermal cycle. In particular, the treatments seemed to influence especially the austenitic areas undergoing transformation and their rate of transformation, the sizes and the more or less acicular morphology of structural elements. In some samples, the presence of tempered martensite and / or bainite was found too.

Keywords:
Q&P steels, quenching, partitioning, retained austenite, mechanical properties

INTRODUCTION

In recent years, a new "concept" of steel called "Quenching and Partitioning" (Q&P), that is innovative from the point of view of chemical composition and of heat treatment is developing. The aim is to produce steels where significant fractions of properly localized retained austenite are present in a martensitic matrix. Q&P belong to the family of AHSS high strength steels (Advanced High Strength Steels). The research on Q&P is still in progress and the first results suggest the possibility of obtaining steels with interesting mechanical properties to provide greater safety in the automotive field and energy saving. This corresponds to the increasing demand by car producers for steels with tensile strength above 1200MPa associated to high ductility.
These high mechanical properties generally require alloyed steels that are very expensive and may increase the vehicle weight. Q&P steels, containing a small amount of alloying elements, could decrease raw materials cost and vehicle weight, thus reducing fuel consumption and therefore carbon dioxide emissions.
Through the thermal treatment, high strength steels (tensile strength greater than 1000-1200MPa) with good ductility can be obtained. The partitioning of carbon from supersaturated martensite into the residual austenite represents the basic process [1- 11].
The function of martensite is to enhance the tensile properties, while the retained austenite increases the elongation (TRIP effect). Its presence among platelets of martensite, improves the possibility of grain boundaries to hinder dislocation movement, thus increasing the resistance. The quenching and partitioning treatment is schematized in Figure 1.
The treatment involves heating the steel to a temperature suffi-

E. Pastore, S. De Negri, M. Fabbreschi,
M.G. Ienco, M.R. Pinasco, A. Saccone
Dipartimento di Chimica e Chimica Industriale,
Sezione di Chimica Inorganica e Metallurgia, Università di Genova
Corresponding author : metal@chimica.unige.it

R. Valentini
Dipartimento di ingegneria chimica, chimica industriale e scienza dei materiali Università di Pisa

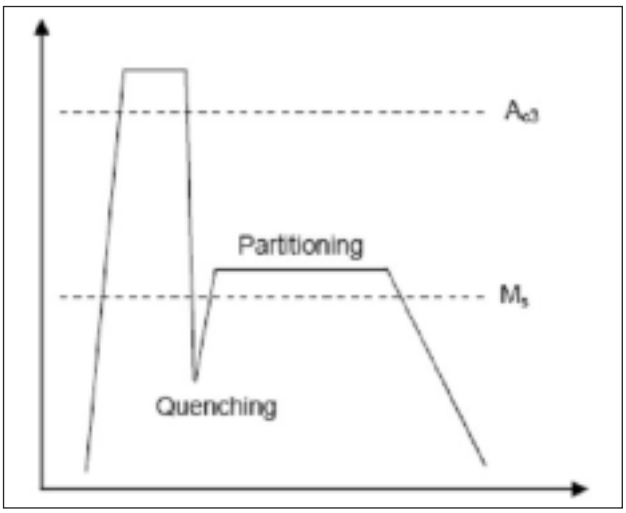

FIG. 1 ***Q&P thermal treatment typical scheme.***
Schema di un tipico trattamento termico Q&P.

Steel type	C	Mn	Si
Bars	0,35	1,3	0,74
Plates	0,19	1,46	1,63

TAB. 1 ***Typical composition of Q&P steels for bars and sheets.***

Composizione tipica di un acciaio Q&P per barre o lamine.

C	Mn	Si	Mo	Al	P	S
0.217	1.647	1.628	0.003	0.005	0.015	0.014

TAB. 2 ***Composition of studied Q&P steel.***

Composizione nominale dell'acciaio Q&P in esame.

cient to have a full austenitization or a mixed structure of ferrite and austenite (heating in the intercritical field). Then, the material is quenched at a temperature QT between Ms and Mf, in order to obtain controlled amounts of martensite and austenite. A partitioning treatment follows at a temperature PT for some time, until the diffusion of carbon takes place, causing the austenite stabilization at room temperature. At the end, fast cooling to room temperature stabilizes the obtained microstructure. The classic tempering treatment, instead, involves the precipitation of carbon from the supersaturated solution as carbides.
Different products, e.g. bars (medium carbon steels) and plates for automotive industry, require different Q&P steel compositions.
The most frequent compositions, found in literature, are shown in table 1.
The carbon content must be high enough to allow the partition process; in the case of plates, a compromise between C content and material weldability is required.
The typical manganese content of a Q&P steel is around 1,4% to ensure sufficient hardenability to the piece; Si, as Mn, increases the steel hardenability by reducing the critical cooling speed.
The Si content, in Q&P steels, is between 0.74%, in the case of steels for bars, and 1.63% for plates. A fundamental property of Si, is to increase the temperature of beginning cementite precipitation in ferrite. The consequent delay in cementite formation facilitates the partition phenomenon.

MATERIALS AND METHODS

The material studied, identified as Si steel, has the typical composition of a Q&P steel for plates (Table 2)
The steel was subjected to the thermal cycles (carried on the Gleeble 3800 thermomechanical simulator), as detailed in table 3 and in figures 2 and 3.
The samples, taken from tensile bars, were embedded so as to observe the longitudinal flat surface, prepared for metallographic examination by the usual mechanical polishing methods and etched with 0.5% nital. Some colour tint etchings for multiphase steels were experimented, but, due to the small size of microstructural elements, no significant information was obtained [6] [12].
The microstructure was investigated by optical and scanning electron microscopy (SEM). The phases present were identified by electron back scattered diffraction (EBSD); the volume fraction of retained austenite at room temperature was measured by X-ray diffraction; and HV hardness measurements were performed. Some mechanical properties were measured by tensile tests.
Transmission electron microscopy (TEM) examinations are in progress.

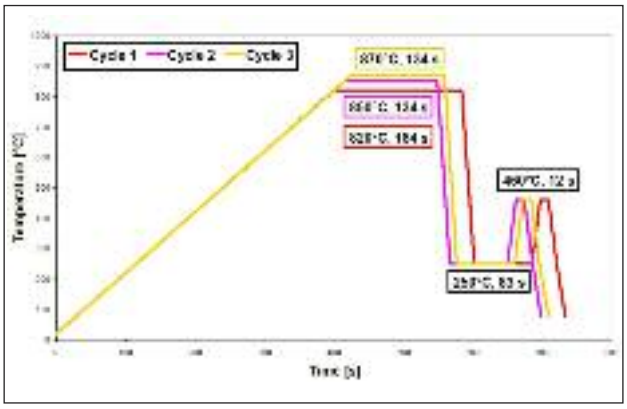

FIG. 2 ***Schematic representation of cycles 1, 2 and 3 (Quenching temperature = 250 °C).***

Rappresentazione schematica dei cicli 1, 2 e 3 (Temperatura di tempra = 250 °C).

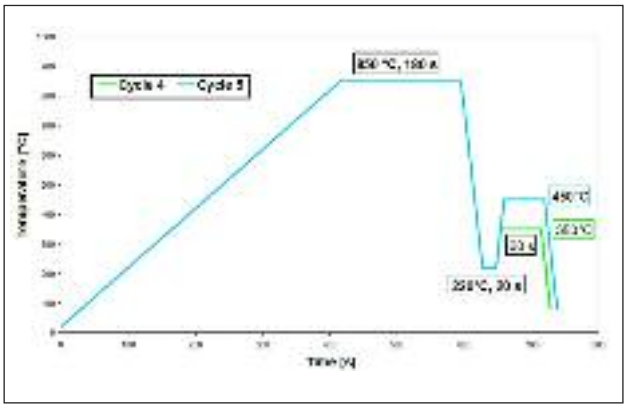

FIG. 3 ***Schematic representation of cycles 4 and 5 (Quenching temperature = 220 °C).***

Rappresentazione schematica dei cicli 4 e 5 (Temperatura di tempra = 220 °C).

Cycle	Samples codes	Soaking T [°C]	Time [s]	Quenching T [°C]	Time [s]	Partitioning T [°C]	Time [s]
1	QP1	820	184	250	83	460	12
2	QP2	850	134	250	83	460	12
3	QP3	870	134	250	83	460	12
4	QP4	850	180	220	20	350	60
5	QP5	850	180	220	20	450	60

TAB. 3
Thermal cycles of the material studied.

Parametri di trattamento dei cicli presi in considerazione.

EXPERIMENTAL RESULTS

Microstructural characterization

The microstructure of the samples subjected to cycles 1, 2 and 3 is very tiny and complex and only at high magnifications it is possible to distinguish several phases. No substantial differences exist among samples (figure 4 and 5). Only for cycle 3 the microstructure is generally more acicular (figure 6).Morphologically different phases were identified through electron microscopy:

- lath martensite in the form of plates with rounded edges or sticks with the same orientation. In some cases, martensite appears as alternating platelets with "retained" austenite/ ferrite/ bainite (figure 7)
- ferrite, where sometimes carbides are present (figure 7)
- more or less extensive areas of austenite undergoing transformation into lath martensite plates with different transformation rates (figure 7).

In QP1 sample, martensite is mainly in form of plates (figure 8) and, only in some areas, it appears with stick morphology (figure 9). Areas of "retained" austenite are quite large (figure 10) and only partially transformed into martensite plates. (figure 11).

In the QP3 sample different morphologies of martensite are clearly visible (figure 12 and 13). In some areas morphological features suggesting tempered martensite are observed (figure 14 and 15).

"Retained" austenite areas are fewer and smaller (than those of QP1) (figure 14) and at an advanced transformation mainly into plate martensite (figure 15).

QP4 and QP5 samples, different from the previous ones in particular for quenching and partitioning temperatures, have a microstructure with the same phases already seen after cycles 1,2 and 3.

In the QP4 sample, the observation by optical microscopy shows closely interconnected areas of austenite with an high transformation rate (figure 16); the austenite transformation rate in the QP5 sample, instead, seems lower and the areas are more defined (figure 17).

By electron microscopy, the austenite in the QP4 sample appears almost completely transformed into martensite plates (figure 18). In some areas are evident areas of tempered martensite (figure 19), and traces of bainite. Packets with alternated platelets of martensite and bainite and / or ferrite are also present (figure 20). The ferrite areas are very limited.

In the QP5 sample martensite appears to have a more stick morphology than plates, austenite has a lower transformation rate (figure 21 and 22) and ferrite is more abundant. Packets with alternated platelets of martensite and bainite are also present (figure 23 and 24). Little carbides in ferrite are observed (figure 25).

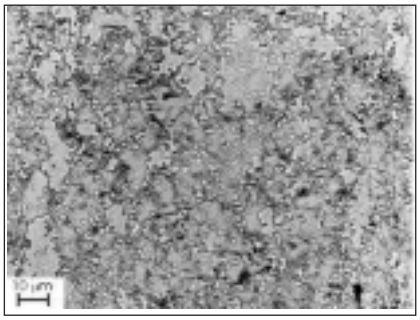

FIG. 4
QP1. MO 1000x, 0.5% nital.
QP1. MO 1000x, 0.5% nital.

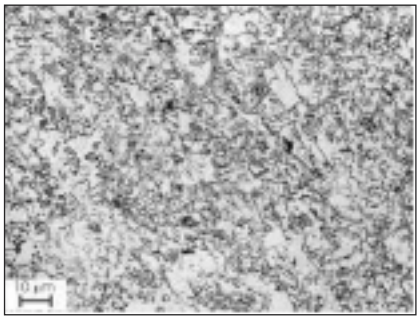

FIG. 5
QP2. MO 1000x, 0.5% nital.
QP2. MO 1000x, 0.5% nital.

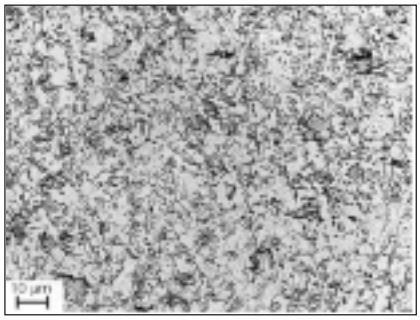

FIG. 6
QP3. MO 1000x, 0.5% nital. The microstructure is essentially acicular.
QP3. MO 1000x, 0.5% nital. Elementi microstrutturali a morfologia tendenzialmente aciculare.

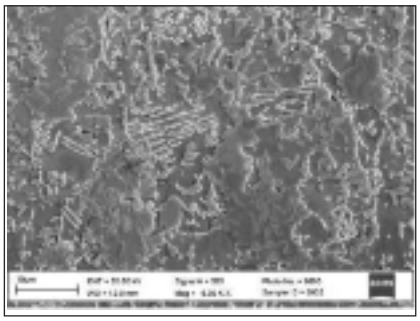

FIG. 7
QP1. SEM 5000x, 0.5% nital. Different phases are evident.
QP1. SEM 5000x, 0.5% nital. Ben visibili le diverse fasi.

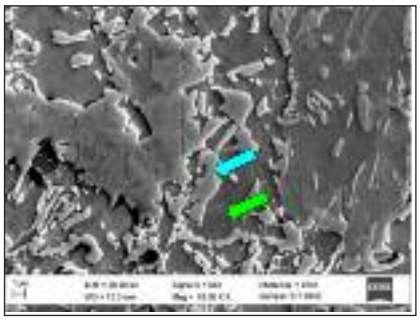

FIG. 8
QP1. SEM 10000x, 0.5% nital. Martensite in form of plates. Respectively light blue and green arrows shows martensite and ferrite.
QP1. SEM 10000x, 0.5% nital. Martensite con morfologia a placche. Le frecce azzurra e verde indicano rispettivamente martensite e ferrite.

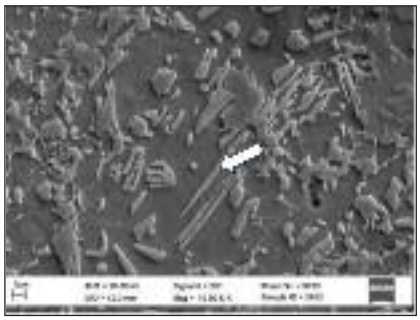

FIG. 9
QP1. SEM 10000x, 0.5% nital. Martensite appears with stick morphology (indicated by arrow).
QP1. SEM 10000x, 0.5% nital. Martensite con morfologia a bastoncelli (indicata dalla freccia).

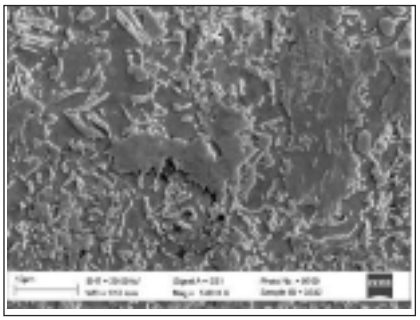

FIG. 10
QP1. SEM 5000x, 0.5% nital. Areas of "retained" austenite are quite large.
QP1. SEM 5000x, 0.5% nital. Aree di austenite "residua".

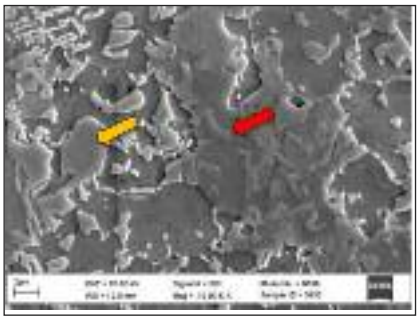

FIG. 11
QP1. SEM 10000x, 0.5% nital. Austenite undergoing transformation into martensite plates (red arrow) and retained austenite (orange arrow).
QP1. SEM 10000x, 0.5% nital. Austenite in via di trasformazione in placche di martensite (freccia rossa) e austenite residua (freccia arancione).

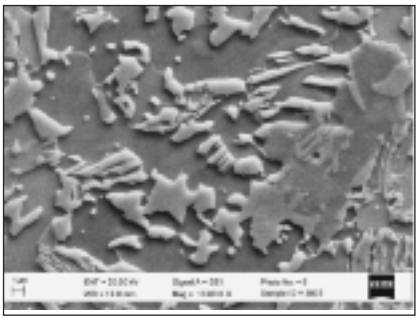

FIG. 12
QP3. SEM 10000x, 0.5% nital. Martensite in form of plates.
QP3. SEM 10000x, 0.5% nital. Martensite a placche.

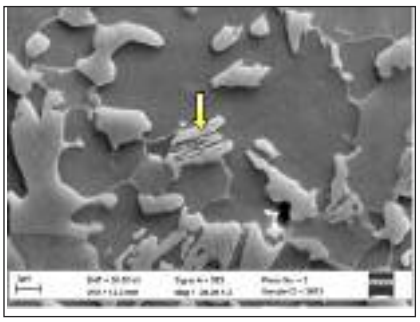

FIG. 13
QP3. SEM 20000x, 0.5% nital. In particular, alternating platelets of lath martensite and retained austenite/ ferrite/ bainite (indicated by arrow).
QP3. SEM 20000x, 0.5% nital. Ben visibili lamelle alternate di martensite lath/ austenite residua/ ferrite/ bainite (indicate dalla freccia).

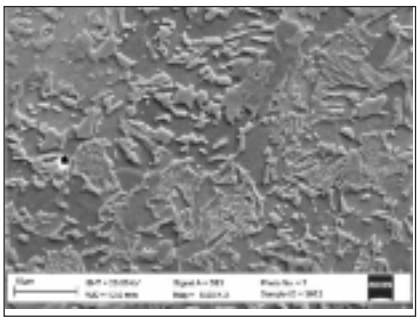

FIG. 14
QP3. SEM 5000x, 0.5% nital. Austenite areas are almost completely transformed.
QP3. SEM 5000x, 0.5% nital. Aree austenitiche ad avanzato grado di trasformazione.

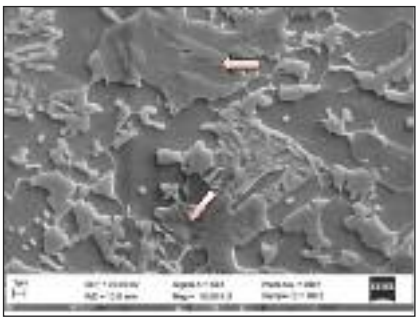

FIG. 15
QP3. SEM 10000x, 0.5% nital. Tempered martensite and "retained" austenite areas undergoing transformation into martensite (indicated by arrows).
QP3. SEM 10000x, 0.5% nital. Martensite rinvenuta ed austenite "residua" in via di trasformazione in martensite (indicata dalle frecce).

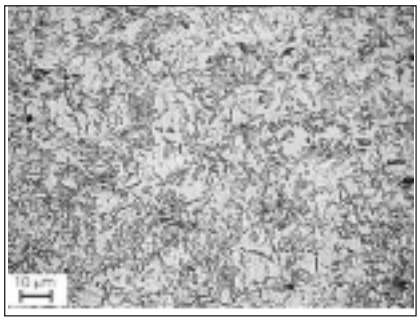

FIG. 16
QP4. MO 1000x, 0.5% nital. Austenite with an high transformation rate.
QP4. MO 1000x, 0.5% nital. Austenite ad alto grado di trasformazione.

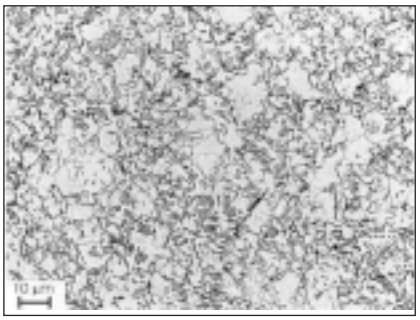

FIG. 17
QP5. MO 1000x, 0.5% nital. Transformation rate is lower.
QP5. MO 1000x, 0.5% nital. Il grado di trasformazione è minore.

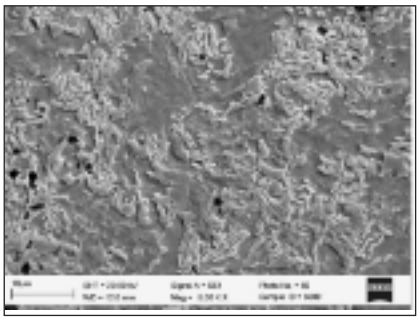

FIG. 18
QP4. SEM 5000x, 0.5% nital. Austenite is almost completely transformed.
QP4. SEM 5000x, 0.5% nital. Austenite quasi completamente trasformata.

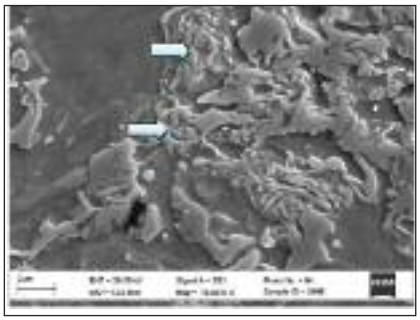

FIG. 19
QP4. SEM 15000x, 0.5% nital. Morphological features suggesting tempered martensite (indicated by arrows).
QP4. SEM 15000x, 0.5% nital. Gli elementi strutturali rimandano a martensite rinvenuta (indicata dalle frecce).

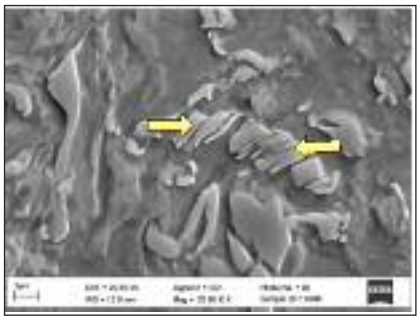

FIG. 20
QP4. SEM 20000x, 0.5% nital. Packets with alternated platelets of martensite and bainite and / or ferrite (indicated by arrows).
QP4. SEM 20000x, 0.5% nital. Pacchetti costituiti da lamelle alternate di martensite e bainite e/o ferrite (indicati dalle frecce).

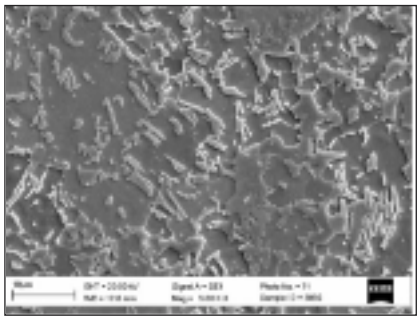

FIG. 21
QP5. SEM 5000x, 0.5% nital. The rods morphology of martensite is evident.
QP5. SEM 5000x, 0.5% nital. Morfologia a bastoncelli della martensite.

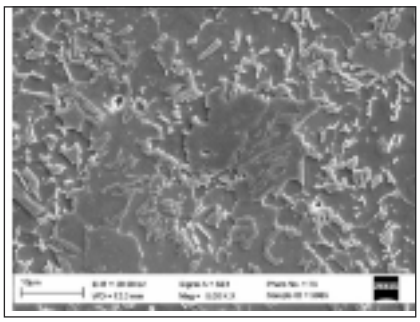

FIG. 22
P5. SEM 5000x, 0.5% nital. The "retained" austenite is little transformed.
QP5. SEM 5000x, 0.5% nital. L'austenite "residua" è poco trasformata.

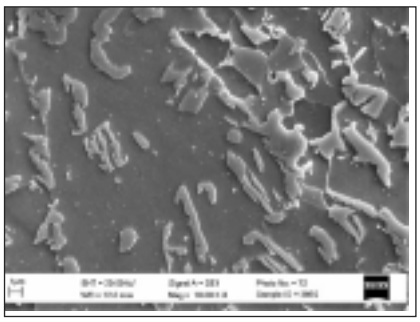

FIG. 23
QP5. SEM 10000x, 0.5% nital. Detail of Fig. 21.
QP5. SEM 10000x, 0.5% nital. Particolare della Fig. 21.

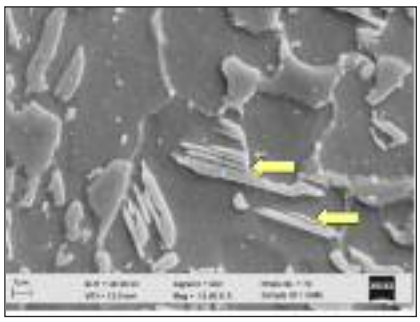

FIG. 24
QP5. SEM 15000x, 0.5% nital. Packets with alternated platelets of martensite and bainite (indicated by arrows).
QP5. SEM 15000x, 0.5% nital. Pacchetti costituiti da lamelle alternate di martensite e bainite e/o martensite rinvenuta (indicati dalle frecce).

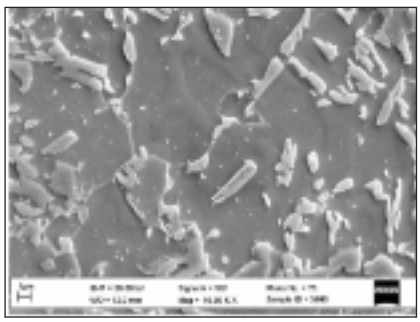

FIG. 25
QP5. SEM 10000x, 0.5% nital. Ferrite, martensite and carbides.
QP5. SEM 10000x, 0.5% nital. Ferrite, martensite e carburi.

ELECTRON BACKSCATTERED DIFFRACTION

In order to support the identification of the phases of the microstructures showed in Fig 8,9,11 an EBSD point analysis was performed on several samples: the results confirmed as noted earlier.

A more complete EBSD analysis was performed on the QP3. (Tsoaking: 870°C, QT:250°C, PT: 460°C).

Figure 26 shows a scanning electron microscopy image of the EBSD scan displayed in Figure 27. In particular, Figure 27 is a combined Image quality map (showed in Fig. 28) and color-coded phase map, in which red corresponds to bcc lattice, green corresponds to fcc lattice, and darker areas correspond to a very low BC, most probably revealing martensite.

Retained austenite morphology is mainly observed as a thick film localized close to martensite along the ferrite boundaries. Some grains show an equiaxes morphology.

Another zone of analysis of the same sample is shown in Fig. 29-30.

In this case the low BC martensitic area (darked red zone) reve-

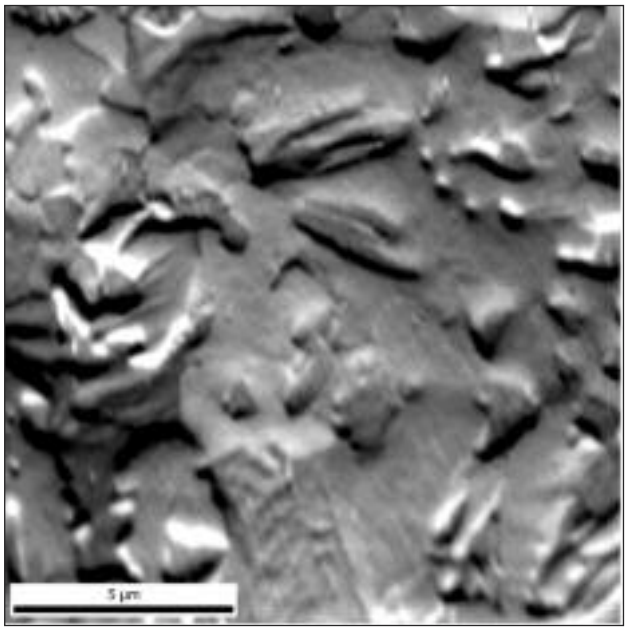

FIG. 26
QP3. SEM EBDS 12000x. Secondary electron image of the scan analysis area.

QP3. SEM EBDS 12000x. Immagine in elettroni secondari della zona di analisi.

FIG. 27
QP3. EBDS 12000x. Combined image quality map and color coded phase map corresponding to the scan shown in Fig X: red colour corresponds to BCC lattice while green identifies FCC lattice. The darker red areas correspond to a very low BCC, most probably revealing martensite.

Fig. 27. QP3. EBDS 12000x. "Image quality map" sovrapposta alla mappa "color coded phase" relativa alla Fig. 26: in rosso il reticolo BCC, il verde identifica il reticolo FCC. Le aree più scure corrispondono ad BCC distorto (very low), molto probabilmente martensite.

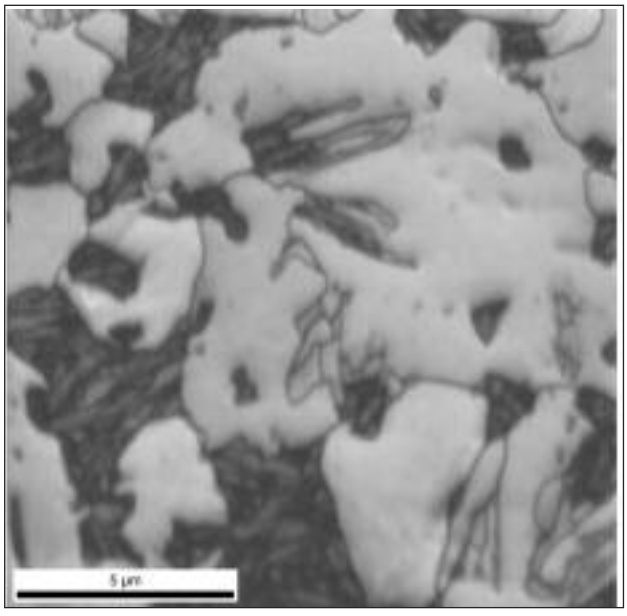

FIG. 28
QP3. EBDS 12000x. Image quality map of the analysed zone shown in Fig 26.

QP3. EBDS 12000x. "Image quality map" della zona analizzata, mostrata in Fig. 26.

als a fine structure: many different plates of martensite are present as clearly revealed by unique color grain map of the same area shown in Fig 31.

HARDNESS MEASURES

The HV1 hardness (load: 1 kg) average values for the different samples are shown in table 4.

Each value is obtained averaging 5 measures (all of them giving less scattered values). The hardness values are very similar in the QP1, QP2 and QP3 samples.

The maximum and minimum value (276 versus 244) belong to the QP4 and QP5 samples.

Samples codes	Hardness (HV1)
QP1	272
QP2	270
QP3	261
QP4	276
QP5	244

TAB. 4
HV1 measures.

Tabella 4. Misure di durezza HV1.

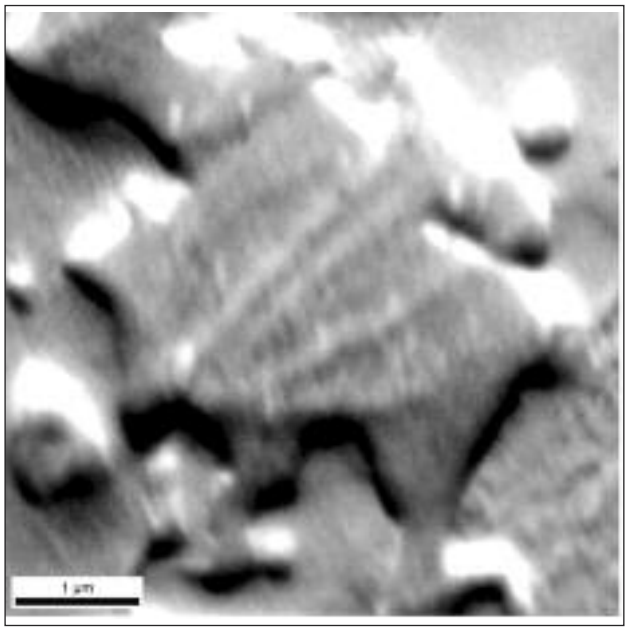

FIG. 29
QP3. EBDS 20000x. Secondary electron image of the scan analysis area of Fig 29.

QP3. EBDS 20000x. Immagine in elettroni secondari della zona di analisi di Fig 29.

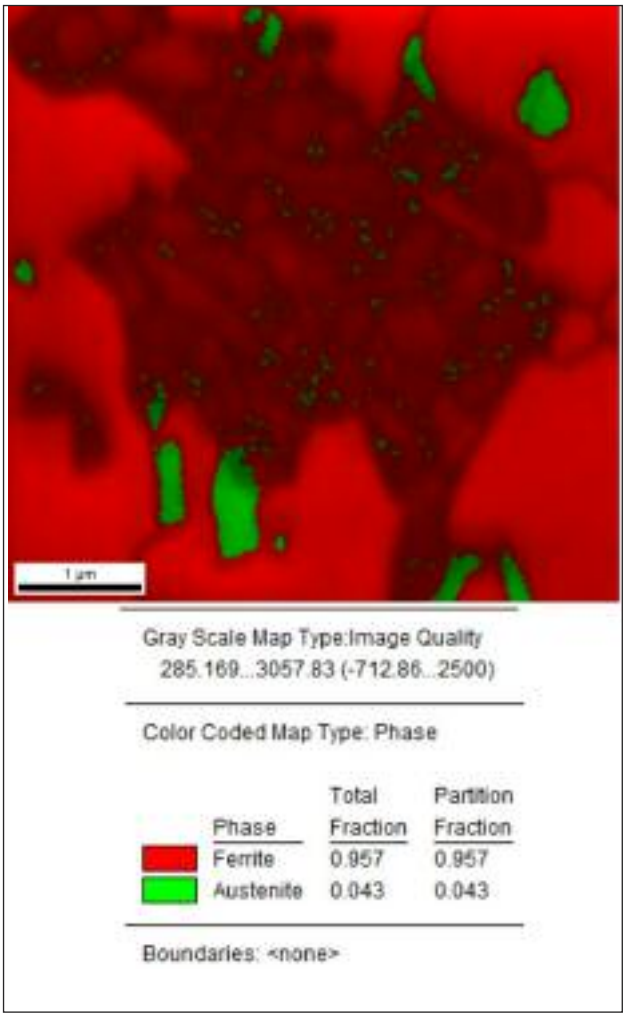

FIG. 30
QP3. EBDS 20000x. Combined image quality map and color coded phase map related to the scan shown in Fig 30.

QP3. EBDS 20000x. "Image quality map" sovrapposta alla mappa "color coded phase" relativa alla zona scansionata di Fig. 30.

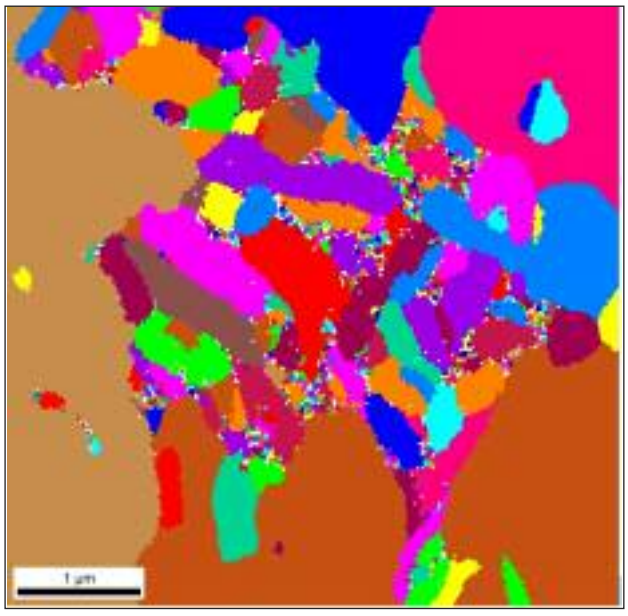

FIG. 31
QP3. EBDS 20000x. Unique color grain map of the scan analysis area of Fig 30.

QP3. EBDS 20000x. "Color grain map" della zona di Fig 30.

MECHANICAL CHARACTERIZATION

Mechanical properties values, obtained by tensile tests, are shown in Table 5.

Rp_{02}, Rm, Rp_{02}/Rm and A% values, related to the different thermal cycles carried out on the material, are compared in figures 32 and 33.

Mechanical tests led to Rp_{02} and Rm values which are not particularly high and to quite low values of Rp_{02}/Rm.

The QP3 sample presents the best compromise between tensile and elongation characteristics. It also provides the greater Rp_{02}/Rm. The QP4 sample exhibits higher Rm than QP3, but

Cycle	$Rp_{0.2}$ [N/mm^2]	Rm [N/mm^2]	Rp/Rm	A [%]
1	362	947	0.38	12.0
2	373	949	0.40	15.3
3	584	1021	0.57	19.3
4	404	1067	0.40	19.5
5	372	938	0.40	22.0

TAB. 5
Mechanical properties values.

Valori delle proprietà meccaniche.

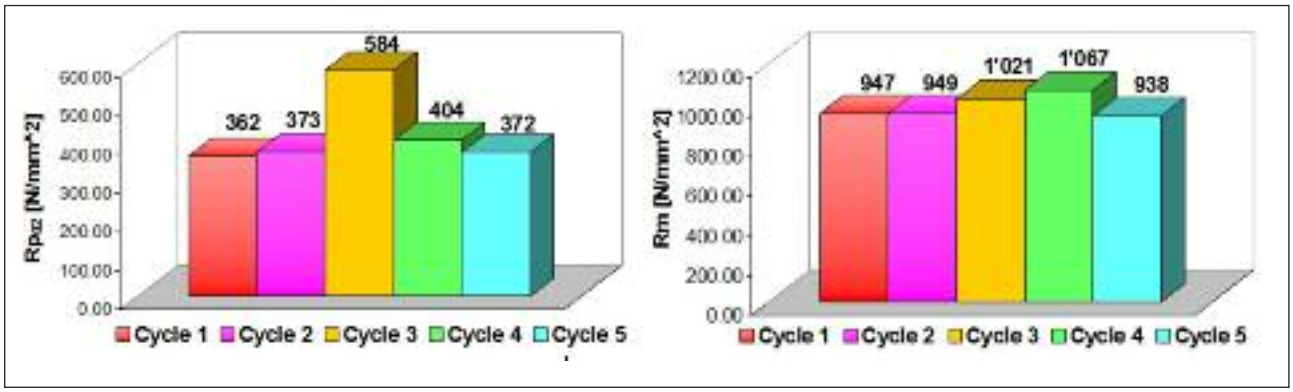

FIG. 32 ***Rp$_{0.2}$ and Rm values.***

Valori di Rp$_{0.2}$ e Rm.

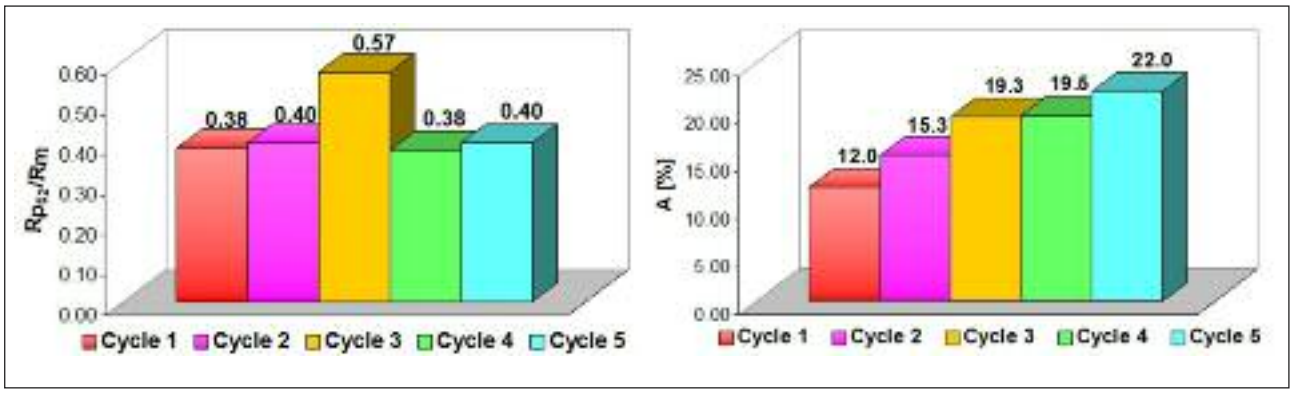

FIG. 33 ***Rp$_{0.2}$/Rm and A% values.***

Valori di Rp$_{0.2}$/Rm e A%.

Rp$_{02}$ is lower (404MPa versus 584MPa) as Rp$_{02}$/Rm value (0.4 versus 0.57). Regarding elongation, the QP5 sample shows the highest value (22%), although its tensile properties are low.

DETERMINATION OF RETAINED AUSTENITE BY X-RAY DIFFRACTION

Retained austenite contents, measured by X-ray diffraction, are given in table 6.

X-ray diffraction (XRD) measurements were performed on a vertical diffractometer X' PertMPD (Philips, Almelo, The Netherlands); a 40 kV voltage and 30 mA current were applied to the X-ray tube, equipped with a Cu anode. Diffraction data were collected in the range 35° ≤ 2 ≤ 120° with steps of 0.03° and a time per step of 3 sec. Samples were analyzed in form of square sheets (1 cm edge) previously stripped in hydrochloric acid.

The integrated intensities (I) of the (200) , (211) , (200) and (311) peaks, measured by means of the FULLPROF program [13], were used to calculate the volume fraction of the retained austenite according to the following formula [14]:

Samples codes	% Austenite
QP1	7.4
QP2	6.4
QP3	6.0
QP4	3.5
QP5	8.1

TAB. 6
Retained austenite fraction.
Frazione di austenite residua.

$$\% \text{ Retained Austenite} = \frac{1}{1 + R_\gamma \left(\frac{I_{(200)\alpha} + I_{(211)\alpha}}{I_{(200)\gamma} + I_{(311)\gamma}} \right)} \cdot 100$$

where: $R_\gamma = \frac{R_{(200)\gamma} + R_{(311)\gamma}}{R_{(200)\alpha} + R_{(211)\alpha}}$

The R factors were calculated according to [15]; the atomic scattering factors were taken after the "International Tables of Crystallography" [16] and the lattice parameters were calculated by a least-squares routine.

In figure 34 the fraction of retained austenite is plotted as a function of soaking temperature.

For the first three cycles, which differ only in the soaking temperature and time, the retained austenite percentage increases slightly as the inter-critical temperature decreases.

Regarding the QP4 and QP5 samples, the varying cycle parameter is the partitioning temperature (350°C for QP4 and 450°C for QP5). The retained austenite fraction amount becomes more than double with increasing partitioning temperature, probably because PT make easier carbon diffusion from martensite to austenite and this phase will be stabilized during the final cooling. It's impossible to compare values of cycle 2, 4 and 5 because the only thermal parameter equal to all is the soaking temperature, but this three samples differ for quenching temperature and time, partitioning temperature and time.

For all cycles tested, we can observe than the retained austenite fraction increase with the partitioning temperature and time, but in particular, the partitioning temperature seems to have more influence than partitioning time.

The highest value of retained austenite about QP5 sample is probably related to the lowest quenching temperature and to the

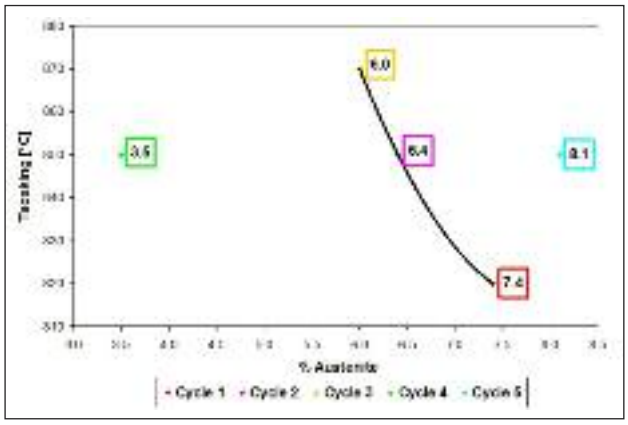

FIG. 34 ***Austenite fraction as a function of soaking temperature.***

Frazione di austenite residua in funzione della temperature di soaking.

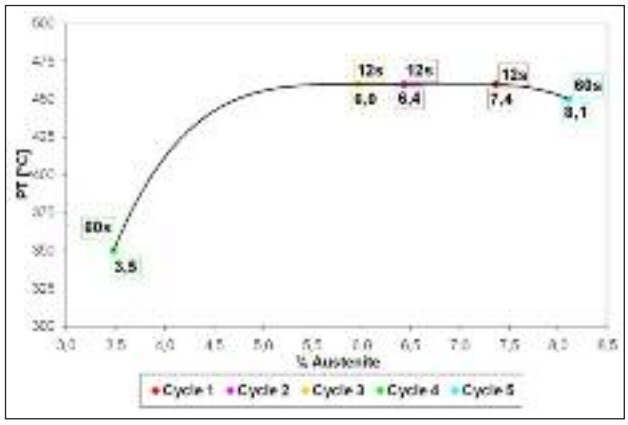

FIG. 35 ***Austenite fraction as a function of partitioning temperature and time.***

Frazione di Austenite in funzione della temperature e del tempo di partizione.

high partitioning temperature and time of all cycles tested [17].

DISCUSSION OF RESULTS

Considering the multiplicity of the phases, the different morphologies presented by the same phase and the different amount and transformation rate of "retained" austenite, it is very difficult to establish a significant correlation among hardness, microstructure and mechanical properties at the present state of research.

However it is possible to observe that:

None of the experimented cycles meet the mechanical properties required of a Q&P steel (Rm > 1000-1200MPa and %A > 10).

QP3 and QP4 sample have similar mechanical characteristics, except for Rp0.2 (584; 404 MPa): the maximum value for QP3 and quite low for QP4.

Considering elongation, cycle 3 provides the best performance, because the higher elongation value (22% for QP5) goes along with significantly lower tensile properties. Concerning the first three cycles, both Rp02 and Rm values are moving upward with increasing soaking temperature, even if a significant increase occurs for a temperature of 870°C (QP3 sample).

About hardness measure, all the values differ little, except the minimun value of QP5 sample (244), according to the microstructure where there are a lot of tempered martensite, and according to the highest value of retained austenite (8.1%) measured by X-ray diffraction. About mechanical properties, at the lowest hardness value (244 for QP5 sample) corresponds the lowest Rm value (938MPa) while at the highest hardness value (276 for QP4 sample) corresponds the highest Rm value (1067MPa). Considering the first 3 cycles, the QP1 and QP2 samples presenting similar hardness (272 – 270) have also similar Rm (947MPa – 949MPa). In the QP3 sample it is not possible to establish a relation hardness - Rm; in fact at slightly lower hardness value (261) corresponds to an higher Rm value (1021 MPa).

SEM analysis pointed out two different aspects of austenite: wide islands and finer thin platelets, this one is often found alternating with martensite platelets. The study of finest austenite is in progress by TEM.

In particular, the best balance of mechanical characteristics are shown in sample QP3, followed by QP4; them microstructure is rich in alternated platelets of austenite/ferrite and martensite.

It's impossible to measure little areas of retained austenite by X-Ray diffraction, it's possible to correlate the retained austenite fraction and the microstructure only if areas of retained austenite are quite large. As regards retained austenite fraction of QP4 (3.5%) and QP5 (8.1%) samples (they differ only for PT), the large percentage change of retained austenite is due to the high transformation rate of austenite in QP4 sample, as is evident in the microstructure(figure 18).

Also in the QP1 (7.4%) and QP3 (6.0%) samples, there is agreement between microstructure and retained austenite fraction. In fact in the QP3 sample, austenite areas are smaller and show a high transformation rate (figure 14).

Concerning mechanical properties, it is possible to establish a trend between retained austenite fraction and Rm. The tensile strength increases (although not proportionally) with decreasing of retained austenite fraction. Rp02 and elongation, cannot be related with retained austenite fractions; in fact very different austenite values led to similar measures of Rp02 and A%.

It should be noted that the X-ray diffraction technique used estimates the whole retained austenite, but only the austenite in packets with martensite seems useful for the "Q&P effect"; probably the common interface make easier carbon diffusion.

CONCLUSIVE CONSIDERATIONS

The phases present in the microstructure are mainly ferrite, "untransformed" austenite and lath martensite. EBSD confirmed observations by scanning electron microscope. The morphology and the relative amounts of these may vary according to thermal cycles. In particular, the treatments seems to influence especially the rate of transformation of austenitic areas, the sizes and the more or less acicular morphology of structural elements. In some samples the presence of tempered martensite and / or bainite was found, too.

For all experimented treatments the steel has provided not quite satisfactory mechanical properties in terms of high strength steels.

The QP3 sample presents the best compromise between tensile and elongation characteristics.

At the present state of research, the multiplicity of the phases, the different morphologies presented by a same phase and the amount and different rate transformation of "retained" austenite, make it very difficult to significantly correlate hardness, microstructure and mechanical properties.

It should be noted that the X-ray diffraction technique used estimates the whole retained austenite, not only the austenite useful for the "Q&P effect".

REFERENCES
[1] Jong-Won Jin, Sang Ho Byun, Seung Il Kim, Chang Seok Oh, Namyun Kang e Ayung-mox Cho "Mechanical Properties Comparison of DP, TRIP, Q&P steels as a function of heat treatment condition", International Conference of new developments in Advanced High-Strength Sheet Steels
[2] D. Matlock, V.E. Brautigam and J. G. Speer "Application of the Quenching & Partitioninig (Q&P) Process to a Medium-Carbon, High-Si Microalloyed Bar steel", Materials Science Forum Vols. 426-432 (2003) pp 1089-1094
[3] J.G. Speer, F. C. Rizzo Assuncao, D. K. Matlock, D. V. Edmonds "The "Quenching and Partitioning" Process: background and recent progress", Material Research vol.8 no.4 417-423, 2005.
[4] C. Fojer, Amy J. Clarke, J. G. Speer "Alloy design for enhanced austenite stabilization via quenching and partitioning", International Conference on new developments in Advanced High-Strenght Sheet Steels 199-207
[5] J. G. Speer, D. V. Edmonds, F. C. Rizzo, D. K. Matlock "Partitioning of carbon from supersatured plates of ferrite, with application to steel processing and fundamentals of the bainite transformation", Current Opionion in Solid State and Materials Science 8 (2004) 219-237
[6] M. Santofimia, L. Zhao, R. Petrov, J. Sietsma "Charaterization of the microstructure obtained by the quenching and partitioning process in a low carbon steel", Material Charaterization 59 (2008) 1758-1764
[7] D.V. Edmonds, K He, M. Miller, F. Rizzo, A.Clarke, D. Matlock and J.G. Speer "Microstructural features of Quenching and partitioning: a new martensitic steel heat treatment" Materials Science Forum Volume 539-543 pag. 4819-4825
[8] A. Clarke, J Speer, M. Miller, R. Hackenberg, D. Edmonds, D.Matlock, F. Rizzo, K.Clarke, E. De Moor "Carbon partitioning to austenite from martensite or bainite during the quench and partitioning process: a critical assessment" Acta materialia 56 (2008) 16-22
[9] Sung Kim, J. Speer, Han Kim, B. De Cooman "Kinetics of phase transformation during Q&P processing" International Conference on New Developments in advanced High strength steels
[10] M. Santofimia, T. Minh, L. Zhao, D. Hanlon, Theo Kop, J. Sietsma "Experimental investigation of quenching and partitioning on two low - carbon steels with different Silicon content" International Conference on New Developments in advanced High strength steels
[11] C. Zhao, D. Tang, H. Jiang, S. Zhao, H. Hui "Process simulation and microstructure analysis of low carbon Si-Mn quenched and parttioned steel" Journal of iron steel research, International (2008) 15(4) 82-85
[12] A. K. De, J. Speer and D. Matlock "Color tint-etching for multiphase steels" Advanced Materials & Processes - February 2003
[13] J. Rodriguez-Carvajal, FULLPROF SUITE, LLB Sacley and LCSIM Rennes, France, 2003.
[14] G. Berti, M. Vaccari, E.Tolle, M. D'Acunto, F. De Marco, "Standard tecnici per la diffrazione a raggi X", Associazione Italiana per l'Analisi delle Sollecitazioni (AIAS)-XXXI Convegno Nazionale-18-21 set tembre 2002, Parma.
[15] B.D. Cullity, Elements of X-ray diffraction, Addison-Wesley, London (1978) p.392.
[16] E. Prince (Ed.). International Tables for Crystallography, Vol. C: Mathematical, Physical and Chemical Tables. Kluwer Academic Publishers, Dordrecht, 2004, p. 557.
[17] S. S. Nayak, R. Anumolu, R. D. K. Misra, K. H. Kim, D. L. Lee, " Microstructure-hardness relationship in quenched and partitioned medium-carbon and high-carbon steels containing silicon", Materials Science and Engineering A 498 (2008) 442-456.

Abstract

Studio di un acciaio Q&P (Quenching and Partitioning) a basso tenore di carbonio

Parole Chiave: acciaio, trasform. di fase, tratt. termici, caratteriz. materiali, processi

Negli ultimi anni, l'industria automobilistica ha volto l'attenzione allo sviluppo di veicoli leggeri, con ridotto impatto ambientale, minor consumo di combustibile e maggiore resistenza agli urti. Tali proprietà appartengono a materiali con alta resistenza a rottura e tenacità, associate ad una buona deformabilità, caratteristiche non ottenibili con i tradizionali acciai al carbonio, nei quali ad un aumento di resistenza corrisponde una diminuzione di duttilità.
Recentemente, è in via di sviluppo una nuova classe di acciai alto resistenziali (AHSS), denominata "Quenching and Partitioning" (Q&P), innovativa dal punto di vista della composizione e del trattamento termico, volta ad ottenere carico di rottura superiore di 1000-1200 MPa e allungamento totale superiore al 10%.
Il trattamento termico prevede la formazione di quantità opportune di martensite ed austenite arricchita di carbonio mediante una tempra fino a temperatura compresa tra Ms e Mf (da campo austenitico o intercritico), seguita da partizione a temperature superiori a Ms. Il processo di partizione dalla martensite, fase sovrassatura di carbonio, all'austenite è la base del processo. Da quanto sopra deriva la necessità di sopprimere ogni reazione competitiva con una composizione opportuna contenente una sufficiente quantità di carbonio ed elementi ritardanti la formazione di carburi quali Si e Al.
Il lavoro rientra in uno studio più ampio avente come tema acciai Q&P (Quenching and Partitioning) sottoposti a differenti cicli termici.
I processi Q&P sono stati condotto mediante un simulatore termomeccanico. Gli acciai in esame sono stati identificati come acciai al Si, Al e Mo. I primi risultati, presentati in questo articolo, riguardano l'acciaio al silicio temprato da diverse temperature (sempre da campo intercritico $\alpha+\gamma$), e partizionato a differenti temperature per diverso tempo di permanenza. Lo scopo di tale trattamento è stato valutare l'influenza dei parametri di processo sulla microstruttura, e di conseguenza, sulle proprietà meccaniche.
La microstruttura è stata osservata mediante microscopia ottica ed elettronica a scansione (SEM); le fasi sono state identificate con electron back scattered diffraction (EBSD); la frazione di austenite residua, a temperature ambiente, è stata misurata con diffrazione RX; sono state eseguite prove di trazione e misure di durezza Vickers. Sono ancora in corso osservazioni al microscopio elettronico in trasmissione (TEM).
Essenzialmente le fasi presenti nella microstruttura di tutti i campioni esaminati sono: ferrite, martensite lath ed austenite "residua". La loro morfologia e le quantità relative dipendono dal ciclo termico. In particolare, il trattamento termico sembra influenzare soprattutto il grado di trasformazione delle aree austenitiche, la dimensione degli elementi strutturali nonchè la loro

maggior o minor acicularità. In alcuni campioni è stata osservata anche presenza di martensite rinvenuta e/o bainite.
Considerando il numero di variabili coinvolte nel processo Q&P, l'impossibilità di una variazione sistematica delle stesse, la molteplicità delle fasi nelle diverse microstrutture, la diversa morfologia con cui si presentano, nonché l'austenite residua presente in quantità e grado di trasformazione variabile, ha reso difficoltoso una correlazione semplice e diretta fra misure di durezza, microstruttura e proprietà meccaniche
Tuttavia è stato possibile osservare che:
Nessuno dei cicli sperimentali soddisfa le proprietà meccaniche richieste ad un acciaio trattato Q&P (Rm > 1000-1200MPa, %A > 10). I campioni QP3 e QP4 presentano caratteristiche meccaniche simile, ad eccezione dell'Rp0.2 (584; 404 MPa) che è il massimo valore per il provino QP3, ma piuttosto modesto per il QP4.
Prendendo in considerazione l'allungamento, i cicli 3 e 4 risultano i migliori, poichè il più alto allungamento (22% per il QP5) corrisponde a caratteristiche resistenziali scarse.
Riguardo ai primi tre cicli, si è osservato un andamento crescente dei valori sia dell'Rp0.2 sia dell'Rm all'aumentare della temperatura di soaking, anche se l'incremento più evidente si ha per il campione QP3 (Tsoaking: 870°C).
Per quanto concerne le misure di durezza, non vi sono differenze significative tra i campioni, fatta eccezione per il campione QP5 che presenta la durezza minima (244), in accordo con la microstruttura in cui è presente abbondante martensite rinvenuta, e con la frazione di austenite residua massima (8.1%) misurata coi RX. Riguardo le proprietà meccaniche, alla durezza minore (QP5, HV1 = 244) corrisponde il minore Rm e il massimo A%; il campione QP4, con valore massimo di durezza (276), presenta il più alto carico di rottura (1067 MPa). Considerando i primi tre cicli, i campioni QP1, QP2, con durezza simile (272 - 270), hanno analogo Rm (947 - 949 MPa); non è possibile stabilire una relazione tra durezza e carico di rottura per il provino QP3, in quanto ad una durezza più bassa (261), corrisponde un maggior Rm (1021 MPa).
Le osservazioni al SEM hanno evidenziato la presenza di due differenti aspetti dell'austenite: ampie aree e sottili lamelle, spesso alternate a martensite lath. Lo studio di questi "pacchetti" mediante microscopio elettronica in trasmissione (TEM) è in corso.
In particolare, si è osservato che i campioni con il miglior compromesso di caratteristiche meccaniche (QP3, seguito da QP4) presentavano una microstruttura ricca di "pacchetti" formati da lamelle di austenite/ferrite alternate a martensite.
Tenendo conto del fatto che la diffrazione a RX misura la frazione di austenite residua solo se stabilizzata e non parzialmente trasformata, si spiega la grande variazione osservata nei campioni QP4 (3.5%) e QP5 (8.1%), che differiscono solamente per la PT; infatti, nel provino QP4, la fase è ad avanzato grado di trasformazione, come evidente nella microstruttura (figura 18).
Anche nei campioni QP1 (7.4%) e QP3 (6.0%) la frazione di austenite residua rilevata concorda con la microstruttura: infatti, nel provino QP3, le aree austenitiche sono meno estese e ad avanzato grado di trasformazione (figura 14).
Riguardo le proprietà meccaniche, è possibile correlare la frazione di austenite residua con l'Rm: il carico di rottura aumenta, anche se non proporzionalmente, con il diminuire della frazione di austenite residua. Il fatto che a valori analoghi di limite di snervamento e allungamento corrispondano differenti quantità di austenite, rende impossibile la correlazione con i risultati dei RX.
Ai fini dell'"effetto Q&P", sembra che particolare importanza abbia l'austenite costituente i cosiddetti "pacchetti", che interfacciandosi alla martensite probabilmente si arricchisce più facilmente di carbonio; peraltro tali piccole aree non sono evidenziabili dalla diffrazione a RX, che stima la quantità totale di austenite residua presente nella microstruttura.